A Numerical Study of an Interacting Particle System

End of Year 1 Report

Thomas M. Hodgson

2020-05-15

Contents

Preface

This report is available in two versions: html and pdf. The pdf version is a traditional static report complied in LaTeX whereas the html version allows for the addition of animations describing the motion of the particles in the systems. Generally, these allow for a much more intuitive view of whats happening, rather than relying on one-dimensional plots. If you're on the html version and would

like the pdf version, simply clock on the Adobe Reader logo in the toolbar at the top of this page (or indeed on any page). It was created using Bookdown [1].

1 Introduction

The physical world is filled with systems of interacting agents, from the nanoscale of atomic interactions to terascale if galaxies filled with stars all exerting a force on one another. Such systems are not limited to physics, nature also provides many examples of complex emergent behaviour such as the slime mould, *Dictyostelium*, which in times of hardship coalesce to form slugs consisting of thousands of individuals to move quickly towards food supplies [2]. Even human behaviour can be seen through this lens: traffic jams, opinions and segregation can all be thought of as interacting particle systems [3, 4]. Although in the physical world the laws governing these systems are generally well understood, the same cannot be said of the biological world where common events like animal migration are still yet to be explained. By viewing these phenomena as interacting particle systems, we aim to codify these interactions and recreate the emergent behaviours *in silico*. This, in combination with an analytical approach, will lead to better understanding of these complex events.

Many attempts have been made to explain the mechanics of these systems, and they broadly fall in to two categories: kinetic models and particle models. Particle models, also known as agent-based models, are favoured by many as they are simple to create and simulate. One can easily develop a set of rules to be followed by individuals and then simulate the behaviour of a group. This was done to great effect by Ballerini et al. who were able to recreate the behaviour of a flock of starlings using very few rules [5]. Kinetic models on the other hand, aggregate the behaviour of individuals into a single partial differential equation. It is this averaging across particles that has seen this method be of great use in statistical mechanics. However, when the interaction between particles becomes more complex, so too does the corresponding PDE which often becomes nonlocal and nonlinear.

These methods are not mutually exclusive. In particular, one can obtain a kinetic model from a particle system (subject to certain conditions) by taking the limit as the number of particles goes to infinity. The methods are thus inextricably linked, however the behaviour of the two can be markedly different. +++ref?+++ In this report we will begin to look at the differences that arise in these two approaches by focussing on one such model: that of Butta et al. [6]. We are particularly interested in the longtime dynamics of this model. The report is structured as follows:

In Section 2 we review some relevant literature in the field, and set up notation.

In Section 3, we present some results on the longtime dynamics of the model.

In Section 4, we numerically simulate two models and compare their behaviour.

In Section 5, we describe the implementation of these simulations.

In Section 6, we suggest directions for our future research.

2 Literature Review

One of the classic studies into collective motion was the work of Vicsek et al. [7] in which what is now known as the Vicsek model was proposed. This is a particle model which exhibits phase transitions despite having a very simple setup. In this model, the particles align themselves based on the average velocities of all the other particles in the system. Every particle has the same speed, and at each timestep the direction, θ is update according to the follwing rule:

$$\theta(t + \Delta t) = \langle \theta(t) \rangle_R + \Delta\theta.$$

Here, $\langle \theta(t) \rangle_R$ denotes the average direction of the velocities of all particles within a distance R of the iˆth particle. The term $\Delta\theta$ is a random variable uniformly distributed on $[-\eta/2, \eta/2]$. With only three free parameters for a given system size (noise η, system density ρ and speed of particles), this model seems very simple. However, it was shown that the system exhibits a phase transition between ordered and unordered motion. This model was designed to be simple, and incorporates some unphysical characteristics such as a hard interaction cutoff and constant particle velocity. Other models have also been proposed, such as the Cucker-Smale model which removes these two restrictions [8].

Both these models have focussed on capturing the essence of interacting particles and do not aim to emulate nature. This allows for analysis and strict bounds to be given on phase transitions. Others have approached the problem from a more biological slant. Through studying natural systems, biologists can develop logical rules for interaction. Couzin et al. follow this approach in developing their model [9].

So far we have been focussing on a one-dimensional analogue of the Vicsek model, sometimes called the Czirok model (after [10]), that was recently analysed by Garnier et al. and a more complex extension developed by Butta et al. [6, 11]. This reduction to one dimension does not make the analysis any easier, in fact in this model the difficulty lies in the interaction term, as we will see. In the remainder of this section we will summarise the contents of these two papers and present some related theory on the longtime behaviour of particle systems.

2.1 A Non-linear Kinetic Model of Self-Propelled Particles with Multiple Equilibria, 2019

In [6], the authors aim to provide a mathematically rigorous explanation of the ordering and symmetry breaking in one dimension seen earlier in [10]. They consider a system of N interacting particles evolving on the one-dimensional torus. For each $i \in \{1, \dots, N\}$, they denote by $x_t^{i,N} \in \mathbb{T}$ and $v_t^{i,N} \in \mathbb{R}$, respectively, the position and velocity of the i-th particle at time t; the dynamics of $x_t^{i,N}$ and $v_t^{i,N}$ is described by the following system of SDEs.

$$\mathrm{d}x_t^{i,N} = v_t^{i,N}\,\mathrm{d}t, \tag{2.1}$$

$$\mathrm{d}v_t^{i,N} = -v_t^{i,N}\mathrm{d}t + G\left(\frac{\sum_{j=1}^N \varphi(x_t^{i,N} - x_t^{j,N})v_t^{j,N}}{\sum_{j=1}^N \varphi(x_t^{i,N} - x_t^{j,N})}\right)\mathrm{d}t + \sqrt{2\sigma}\mathrm{d}W_t^i, \tag{2.2}$$

where the W^i's are independent one-dimensional standard Brownians and $\sigma > 0$ is a given parameter. When the *interaction function* φ is identically equal to one this is a mean field- type model. If the

support of φ is not the whole torus then the interaction is local, i.e. particle i interacts only with the particles within the support of φ. We will refer to G as being the *herding function*. Note here that in the interaction term, the denominator involves other nearby particles.

We will explain the role of G below; for the time being we assume that G satisfies the following

$$G(u) = -G(-u)\,, \qquad \begin{cases} G(u) > u & \text{if } 0 < u < 1\,, \\ G(u) < u & \text{if } u > 1\,. \end{cases} \tag{2.3}$$

In [6] it was shown that, as $N \to \infty$, the empirical measure of the particle system converges to a measure whose density is the solution of the continuum evolution described by the following nonlinear PDE

$$\partial_t f_t(x,v) = -v\,\partial_x f_t(x,v) - \partial_v\big\{\big[G(M_{f_t}(x)) - v\big] f_t(x,v)\big\} + \sigma\,\partial_{vv} f_t(x,v)\,, \tag{2.4}$$

where the nonlinearity M_f is given by

$$M_f(x) := \frac{\int_{\mathbb{T}} \mathrm{d}y \int_{\mathbb{R}} \mathrm{d}w\, f(y,w)\,\varphi(x-y)\,w}{\int_{\mathbb{T}} \mathrm{d}y \int_{\mathbb{R}} \mathrm{d}w\, f(y,w)\,\varphi(x-y)}\,. \tag{2.5}$$

They fully classify the dynamics of this evolution under a space-homogeneity assumption (namely that $\varphi \equiv 1$). Under this assumption, they also formulate a Lyapunov functional and deduce its rate of decay, thereby proving that only three invariant measure exist for this case (See Section 3 for some elaboration).

In the inhomogeneous case, they prove that the equation is well-posed in the weighted $L^1(\sqrt{1+v^2})$ space. They were unable, however, to prove the existence of only three stationary measures. +++Mention that this is one of our aims here?+++ They do show however, that when the interaction is a small oscillation around uniform, that there are only three stationary measures. Further to this, they show that the empirical measure of the particle system in [10] converges to the solution of the kinetic model.

2.2 Mean Field Model for Collective Motion Bistability, 2019

In [11], the authors consider a similar model to [6], with one difference. Instead of scaling by the number of particles local to each agent, they scale by the total number of particles in the system. Although counterintuitive, this is present in many models, as it reduces the convergence of the measure to an easier case, where the interaction is of mean-field type +++is this correct?+++. The dynamics of the particles is given by

$$\mathrm{d}x_t^{i,N} = v_t^{i,N}\,\mathrm{d}t, \tag{2.6}$$

$$\mathrm{d}v_t^{i,N} = -v_t^{i,N}\mathrm{d}t + G\left(\frac{\sum_{j=1}^N \varphi(x_t^{i,N} - x_t^{j,N}) v_t^{j,N}}{N}\right)\mathrm{d}t + \sqrt{2\sigma}\mathrm{d}W_t^i. \tag{2.7}$$

They show that in this case the nonlinearity in the kinetic model (2.4) reduces to (cf. (2.5)):

$$M_f(x) := \int_{\mathbb{T}} \mathrm{d}y \int_{\mathbb{R}} \mathrm{d}w \, f(y,w) \, \varphi(x-y) \, w. \tag{2.8}$$

Similar to [6], they prove the existence of three invariant measures for this equation along with some stability analysis. They also produce numerical simulations of the particle system to confirm their analytical findings. +++ Add more and explain their numerics? +++

In summary, the two models presented in [6] & [11] are very similar, however this discrepancy in the interaction term will in fact have large effects on the dynamics. These are explored further in Section 4

2.3 Other Papers?

To be able to study the longtime dynamics of interacting particle systems, we will need some theory. The majority has been developed for the case when the interaction takes a mean-field form, and the equation can be written in gradient form.

+++ example of system +++

+++ Should I write about Stuart + Mattingly? +++

3 Analysis

The model (2.4) was introduced in [6] and, in a simplified version, in [11] as well. We briefly summarize what is known about the nonlinear evolution (2.4) and then explain the main objectives and results of this paper. When φ is uniformly positive, i.e. $\varphi(x) > \epsilon$ for some constant $\epsilon > 0$, the well-posedness of the PDE (2.4) has been studied in [6]. A complete analytic description of the long-time behaviour of (2.4) seems to be out of reach (we explain below why this is the case); however, the asymptotic behaviour of this dynamics has been characterized in some simplified cases, namely i) when the density f_t is space-homogeneous, i.e. when it does not depend on the space-variable x; ii) when the function φ is a perturbation of the mean field case and iii) when the non- linearity (2.5) is simplified. Let us comment on these three cases in turn.

i) If we consider only space- homogeneous densities, i.e. solutions of the form $f_t(v)$, then the evolution (2.4)-(2.5) reduces to the (much) simpler dynamics

$$\partial_t f_t(v) = -\partial_v \big\{ \big[G(M(t)) - v \big] f_t(x,v) \big\} + \sigma \, \partial_{vv} f_t(x,v) \,, \tag{3.1}$$

where $M(t) := \int_{\mathbb{R}} v \, f_t(v) \mathrm{d}v$ solves the one-dimensional ODE

$$\dot{M}(t) = G(M(t)) - M(t). \tag{3.2}$$

In other words, the nonlinearity $M_{f_t}(x)$ reduces to being the average velocity $M(t)$; because one can close an equation on $M(t)$, one can now regard $M(t)$ as being a time-dependent coefficient; hence, in this spec-homogeneous case, the nonlinear dynamics (2.4) reduces to a linear, non-autonomous PDE. In this case one can easily prove that there exist three stationary solutions of @(eq:lin), namely three Gaussians

$$\mu_\pm = \frac{1}{Z_\pm} e^{-\frac{(v\mp 1)^2}{2\sigma}} \quad \text{and} \quad \mu_0 = \frac{1}{Z_0} e^{-\frac{v^2}{2\sigma}}\,, \tag{3.3}$$

where $Z_\pm$ and Z_0 are appropriate normalization constants. Note that these are the only three stationary solutions of the dynamics @(eq:lin)-@(eq:Mlin), *irrespective of the value of* σ. This feature is unusual for these kind of models, and it is often referred to as *unconditional flocking*. Moreover, if the initial profile f_0 has positive mean, i.e. if $M(0) > 0$ ($M(0) < 0$, respectively) then the dynamics converges exponentially fast to the stationary measure with positive mean, μ_+ (μ_-, respectively).

ii) As we have mentioned, the study of the long-time behaviour of the full model (2.4)-(2.5) is quite challenging. In particular one can easily see that the three measures (3.3) are still stationary solutions of (2.4)-(2.5); however the authors of [6, 11] were not able to prove that these are indeed the only three stationary measures; this is a conjecture that we will confirm numerically in this paper - see Section **??** and Section **??**. The fact that the measures (3.3) are the only stationary solutions of (2.4)-(2.5) has been proven analytically only in the case in which the function φ is chosen to be a small oscillation around the constant function $\varphi \equiv 1$; to be more precise, this has been proven (under some assumptions on the regularity of the solution), only in the case in which

$$\varphi(x) = 1 + \lambda\psi(x), \quad \text{where } 0 < \lambda \ll 1, \int_{\mathbb{T}} \psi(y)\, dy = 0\,.$$

The difficulty in solving the stationary problem associated with (2.4)-(2.5) comes from the fact that such a model is *not* in gradient form.

iii) In [11], the authors introduced a model similar to (2.4)-(2.5), namely they study the following non-linear PDE

$$\partial_t f_t(x,v) = -v\,\partial_x f_t(x,v) - \partial_v\big\{\big[G(\tilde{M}_{f_t}(x)) - v\big] f_t(x,v)\big\} + \sigma\,\partial_{vv} f_t(x,v)\,, \tag{3.4}$$

where this time nonlinearity $\tilde{M}_f$ is given by

$$\tilde{M}_f(x) := \int_{\mathbb{T}} \mathrm{d}y \int_{\mathbb{R}} \mathrm{d}w\, f(y,w)\, \varphi(x-y)\, w\,. \tag{3.5}$$

{Explain here that the difference between the two models boils down to a different choice of normalization. }For such a model they study long time behaviour and stability of the equilibria (3.3), which are shown to be the only stationary states for (3.4).

With this premise in mind, we move on to explaining the content of this paper.

+++ Show particle system invariant measure has mean zero when ($\phi \equiv 1$) +++

We first summarise the relevant PDE results presented in Butt'a et al. [6].

3.1 Product Distribution is a Solution

Consider the stationary problem,

$$-v\partial_x f_t(x,v) + \partial_v v f_t(x,v) - \partial_v\left[G\left(M(t,x)\right) f_t(x,v)\right] + \sigma\partial_{vv} f_t(x,v) = 0. \tag{3.6}$$

Here we will show that a product distribution is a solution of the stationary problem (3.6) if and only if it is uniform in the space variable and Gaussian in the velocity variable. Moreover, the Gaussian velocity can only have variance σ and mean u where u solves $G(u) = u$. Let $f(x, v) = g(x)h(v)$, for some functions g, h. Note the lack of dependence on t as we seek stationary solutions. Then,

$$\begin{aligned}\partial_x g(x)h(v) &= h(v)\partial_x g(x)\\ \partial_v g(x)h(v) &= g(x)\partial_v h(v)\\ \partial_{vv} g(x)h(v) &= g(x)\partial_{vv} h(v)\end{aligned}$$

The averaging function $M(t, x)$ can also be simplified.

$$\begin{aligned}M(x) &= \frac{\int_{\mathbb{T}} \mathrm{d}y \int_{\mathbb{R}} \mathrm{d}w\, g(y)h(w)\phi(x-y)w}{\int_{\mathbb{T}} \mathrm{d}y \int_{\mathbb{R}} \mathrm{d}w\, g(y)h(w)\phi(x-y)}\\ &= \frac{\left(\int_{\mathbb{R}} \mathrm{d}w\, wh(w)\right)\int_{\mathbb{T}} \mathrm{d}y\, g(y)\phi(x-y)}{\left(\int_{\mathbb{R}} \mathrm{d}w\, h(w)\right)\int_{\mathbb{T}} \mathrm{d}y\, g(y)\phi(x-y)} \quad \text{by independence}\\ &= \int_{\mathbb{R}} \mathrm{d}w\, wh(w)\\ &= \langle w\rangle_h\end{aligned}$$

Note here that the average velocity depends on the distribution. Substituting this all in to (3.6) gives,

$$-vh(v)\partial_x g(x) + g(x)\partial_v\left[(v - G(\langle w\rangle))h(v) + \sigma\partial_v h(v)\right] = 0. \tag{3.7}$$

Then, integrating in space,

$$\begin{aligned}&\partial_v\left[(v - G(\langle w\rangle))h(v) + \sigma\partial_v h(v)\right] = 0\\ \implies &\left[(v - G(\langle w\rangle))h(v) + \sigma\partial_v h(v)\right] = \text{const.}\end{aligned}$$

where the first addend is zero by periodicity of the torus. So,

$$\partial_v h - \left(\frac{G(\langle w\rangle) - v}{\sigma}\right)h + \text{const.} = 0.$$

This can be solved using an integrating factor to give

$$h(v) = C\mathrm{e}^{\frac{2G(\langle w\rangle)v - v^2}{2\sigma}}.$$

Applying the normalising constraint gives

$$h(v) = \frac{1}{\sqrt{2\pi\sigma}}\mathrm{e}^{\frac{-(v-G(\langle w\rangle))^2}{2\sigma}}.$$

So the velocity distribution at stationarity is Gaussian with mean $G(\langle w\rangle)$ and variance σ^2. If we take the smooth herding function $G(u) = \frac{\operatorname{atanh}(u)}{\operatorname{atanh}(1)}$, this corresponds to a Gaussian with mean $-1, 0$ or $+1$,

depending on the initial data. Returning to Equation (3.7), we see that the first addend must be identically zero for the equation to hold. In particular, this implies $\partial_x g(x) = 0$, due to the positivity of $h(v)$ (as it is a Gaussian). We thus deduce that g must be the uniform measure on $\mathbb{T}$. Hence, $f_t(x, v) = g_t(x)h_t(v)$ is a stationary solution of the PDE (3.6).

3.2 Convergence Depends on Initial Average Velocity

If we further assume space homogeneity of the PDE, that is, $f_t(x, v) = h_t(v)$, we can infer exactly how the average velocity controls the dynamics. If we multiply the space homogeneous PDE by v and integrate with respect to velocity we obtain

$$\int v\partial_t h_t(v)\mathrm{d}v = -\int v\partial_v G(\langle w\rangle)h_t(v)\mathrm{d}v + \int v\partial_v v h_t(v)\mathrm{d}v + \sigma\int v\partial_v v h_t(v)\mathrm{d}v$$

Integrating by parts then gives an autonomous first order ODE.

$$\partial_t\langle w\rangle = G(\langle w\rangle) - \langle w\rangle$$

As it is autonomous, the solution must be monotone, that is, the average velocity. There are stationary points whenever the average velocity solves $G(\langle w\rangle) = \langle w\rangle$, as expected from the product solution found previously. For example, if we take $G(u) = \frac{\operatorname{atanh}(u)}{\operatorname{atanh}(1)}$, then the average velocity converges to $ -1, 0 $ or $+1$, depending on the sign of the initial average velocity. If $\langle w\rangle|_{t=0} > 0$, then $\langle w\rangle \to +1$. Similarly, the stationary point at -1 is stable and the system will converge there for any configuration such that $\langle w\rangle|_{t=0} < 0$. Finally, 0 is an unstable equilibrium, only attainable when $\langle w\rangle|_{t=0} = 0$. See Figure 1 for a phase plane diagram of the system when G is the inverse hyperbolic tangent.

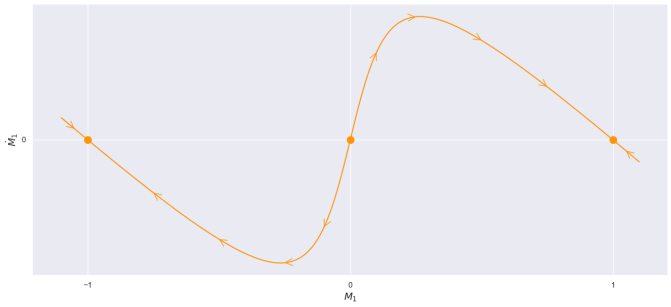

Figure 1: Dynamics of the space homogeneous ODE.

To summarise, there are three key facts gleaned here that we use to predict the behaviour of the particle system.

- The average velocity of the system is monotone (when space homogeneity is assumed).
- The initial average velocity controls the convergence (again, when assuming space homogeneity).
- A product of a Gaussian and a uniform distribution is a solution to the full PDE (when $\sigma \neq 0$)

4 Numerical Studies

What are we trying to do here? Learn more about Butta model, isolate what does what.

4.1 PDE Simulation

Hundsdorfer-Verwer, Extended to two dimensions, started on finite volume, flux limiting. Was slow, moved to DDFT software from BG. Ongoing work to simulate deterministic PDE.

4.2 Particle System Simulation

Results – Initial simulations show as expect Low particle numbers Hitting times Moved to deterministic model:

- Effect of interation function hard cutoff
- Effect of herding function/gradient

4.2.1 Deterministic Model

In this section we will simplify the models by removing the noise term in the velocity equation. Through a series of examples we will show that despite the similarity, these models can behave very differently. This section will also show that although the PDE is the limit of the particle system, knowledge gained in the study of the PDE can not always be transferred. It will also serve as a good insight into the dynamics of the model. We begin with the simplest case: a lone particle given a deterministic initial velocity.

4.2.1.1 One Particle, Deterministic Velocity This is the simplest initial configuration, simply simulating one particle with a deterministic initial velocity:

$$x_0^{1,1} = 0, \qquad v_0^{1,1} = 2$$

The choices here are completely arbitrary, the dynamics will be the same regardless of position on the torus or the velocity. Figure **??** shows that the particle very quickly comes to a stop. This is intuitive from looking at the particle model, but obviously not predicted by the kinetic model. The particle model contains a damping term, while the only forcing arises through the interaction, in the absence of noise. This is because of the $j \neq i$ in the summation within the interaction term.

$$\frac{\sum_{j=1,\, j\neq i}^{N} v_t^{j,N} \varphi(x_t^{j,N} - x_t^{i,N})}{\sum_{j=1,\, j\neq i}^{N} \varphi(x_t^{j,N} - x_t^{i,N})}$$

In fact, this equation doesn't make sense for only one particle as it evaluates to $\frac{0}{0}$. We mitigate this numerically by adding a very small constant to the denominator, so that the term can be evaluated.

This example, while trivial, already illustrates the difference that can arise between kinetic and particle models. (Although, an interacting particle system with only one particle and no interaction is a *slightly* degenerate case.)

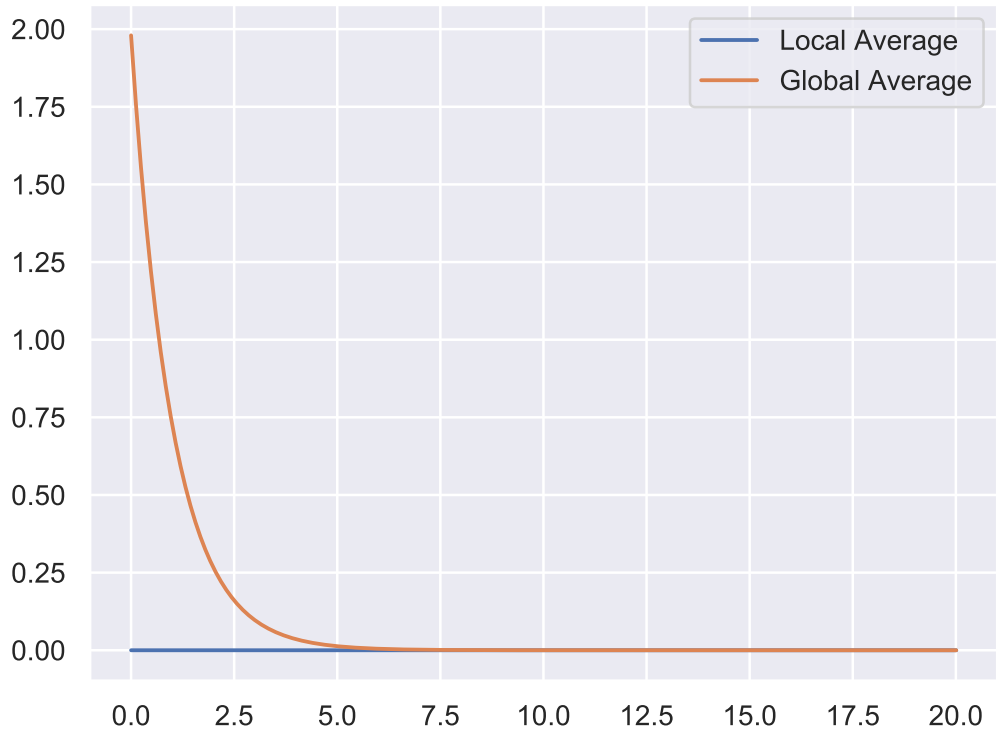

Figure 2: Velocity of one particle that begins with velocity 2 with no noise. See oneparticlestop.mp4

4.2.1.2 Three Particles With three particles in the system, more possible behaviours arise. We configure these particles as follows.

$$x_0^{1,3} = 0 \quad x_0^{2,3} = \frac{6\pi}{100} \quad x_0^{3,3} = \frac{4\pi}{3} v_0^{1,3} = 1.5 \quad v_0^{2,3} = 1 \quad v_0^{3,3} = 0$$

If we use the indicator interaction function,

$$\varphi(x) = \mathbb{1}_{[0,\gamma L]}(\|x\|), \quad 0 \leq \gamma \leq \frac{1}{2}, \tag{4.1}$$

the interaction radius γ determines the convergence of this setup. Here, the system has positive initial average velocity, and as such we expect a monotone convergence to $+1$. Indeed, taking the interaction radius large enough, for example $\gamma = 0.06$, this is exactly what happens. The system coalesces into one cluster travelling at velocity $+1$. Note here that in the absence of noise we expect neither a normally distributed velocity or a uniform distribution in space. However, if we instead take $\gamma = 0.04$, the interaction is not strong enough for the particles to coalesce. One particle is always left behind as the two clustered particles pass by. This causes a periodic average velocity—that is, not monotone, immediately in contrast to **??** above. It is to be expected that an equation derived from the limit as the number of particles tends to infinity does not reflect the behaviour of just three particles.

The problem here is not just that you don't have enough particles (as we have seen, we can obtain periodic behaviour with arbitrarily large number of particles) but also the fact tat we don't know (because we haven't studied it) the behaviour of the limiting equation that you would obtain by sending N to infinity without noise – M

Finally, if the interaction radius is too small, say $\gamma = 0.01$, then the system behaves as the one particle case, with all particles becoming stationary. This is because the fast moving particle passes through the slower particle without having sufficient time to coalesce. Relevant animations for these three behaviours are `3_particle_gamma_{01,04,06}.mp4`

4.2.1.3 Progressively Spaced Next, we arrange the particles so that the distance between them increases linearly. That is the distance between the first two is 1, between second and third is 2, etc. The gaps are then scaled onto the torus. This will allow the control of how many particles initially interact.

Here it seems that there are two possibilities: either the system converges to positive average velocity 1 or a periodic orbit occurs, depending on γ. However, the regime in which γ causes a periodic trajectory also depends on N. For larger N, γ has to become exceedingly small to produce any interesting behaviour. This is because the gap between the first few particles becomes very small.

4.2.1.4 Clusters of Uneven Density The most illustrative example is starting the particles in two diametrically opposite clusters of equal width one containing one third of the total particles with positive velocity, and the other containing two thirds of the particles with negative velocity. This allows for an interesting setup—most particles can move with negative velocity while the average velocity remains positive. We give each particle in the small cluster velocity 1.8, while in the larger cluster all particles have velocity -0.2. The initial average velocity of the system is thus around $+\frac{1}{2}$. The values were chosen so that each cluster is an equal distance from its equilibrium value, were it the only cluster in the system.

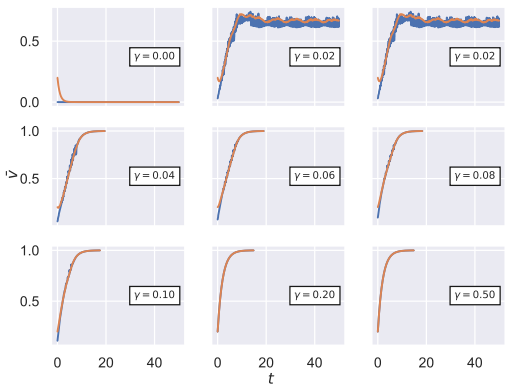

Figure 3: Average velocity of 20 particles progressively spaced with increasing radius of interaction. Note the three different behaviours—the system either converges to $0, +1$ or oscillates. See `prog_spaced_avg_vel_{2,005,010}.mp4`

$$x_0^{i,3N} \sim U\left[\pi - \frac{\pi}{10}, \pi + \frac{\pi}{10}\right], \qquad v^{i,3N} = -0.2 \quad \text{for } 1 \leq i \leq 2N,$$
$$x_0^{i,3N} \sim U\left[-\frac{\pi}{10}, \frac{\pi}{10}\right], \qquad v^{i,3N} = 1.8 \quad \text{for } 2N \leq i \leq 3N.$$

This is the first example that exhibits a clear difference depending on the scaling used in the interaction term. We will use the term *local scaling* to describe the model of [6] with interaction term,

$$M(t,x) = \frac{\sum_{j=1,j!=i}^{N} v_t^{j,N} \varphi(x_t^{j,N} - x_t^{i,N})}{\sum_{j=1,j!=i}^{N} \varphi(x_t^{j,N} - x_t^{i,N})},$$

that is where the interaction is modulated by the number of particles with which each particle is interacting. In contrast, the term *global scaling* describes the model of [11] with interaction term,

$$M(t,x) = \frac{\sum_{j=1,j\neq i}^{N} v_t^{j,N} \varphi(x_t^{j,N} - x_t^{i,N})}{N},$$

where we scale by the total number of particles in the system, irrespective of interaction. Note that if we use the indicator interaction function, (4.1), the local scaling converges to the global scaling as the interaction radius increases, i.e.

$$\sum_{j=1,j\neq i}^{N} \varphi(x_t^{j,N} - x_t^{i,N}) \to N \text{ as } \gamma \to \frac{1}{2}.$$

4.2.1.4.1 Average Velocity Figure 4 shows the average velocity of a wide range of interaction radii and particle numbers. There a few things to note here. First, the interaction radius has complete

control over the convergence. This is in contrast to **??**, the average velocity is not determining the convergence value. Second, the number of particles in the system has no effect on whether the system converges to $+1$ or -1 and a negligible effect on the speed of convergence. Thirdly, the average velocity is not monotone, even for large numbers of particles—in contrast to **??**. This happens for all $0.2 \leq \gamma \leq 0.45$. For $\gamma = 0.05$ we see that the system settles into a periodic orbit, before eventually converging to -1.

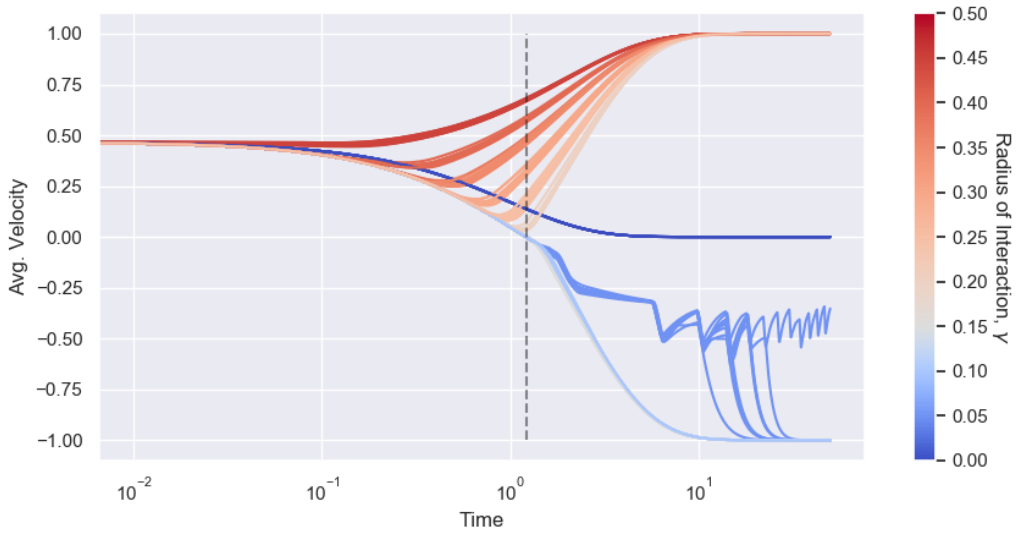

Figure 4: Average velocity of systems for a range of γ. Particle numbers were varied between 24 and 456. Systems were evolved using the Euler-Maruyama scheme applied to the locally scaled model for $50s$ with a timestep of 0.01. This allows enough timesteps for interactions to be resolved. The indicator interaction function was used and a herding function that is symmetric about ± 1. (Note the logarithmic scale). Corresponding animations `Local0.15_N264_neg.mp4`, `Local0.05_N72_periodic.mp4`,`Local0.2_N264_pos.mp4`

This is the first example in which we see a stark difference between the locally-scaled and globally-scaled models. When the systems are evolved for only $50s$, the systems appear to converge to a value dependent on the interaction radius. In fact, these are not stable points and evolving for $500s$ allows the systems to settle to ± 1. See Figure **??**. Periodic, erratic trajectories are also much more prevalent in this model. We also see that some systems do not converge within $500s$, instead remaining in a periodic trajectory. The average velocity time series is not very illuminating here—in the corresponding animations it can be seen that these are the result of one large cluster forming and few particles remaining separate. The cluster is not strong enough to retain these particles as it passes by. The lone particle is then left behind by the cluster where it slows until the next orbit of the large cluster. This is state remains even for $1000s$, see for example `outlier_global_312.mp4`. Irrespective of scaling, once the radius of interaction and the initial data are fixed, both models converge eventually to the same average velocity. We have not observed any regimes in which the globally scaled equation converges to $+1$ while the locally scaled model converges to -1 (or vice versa).

So we see that the space homogeneous PDE and the particle system have very different behaviours,

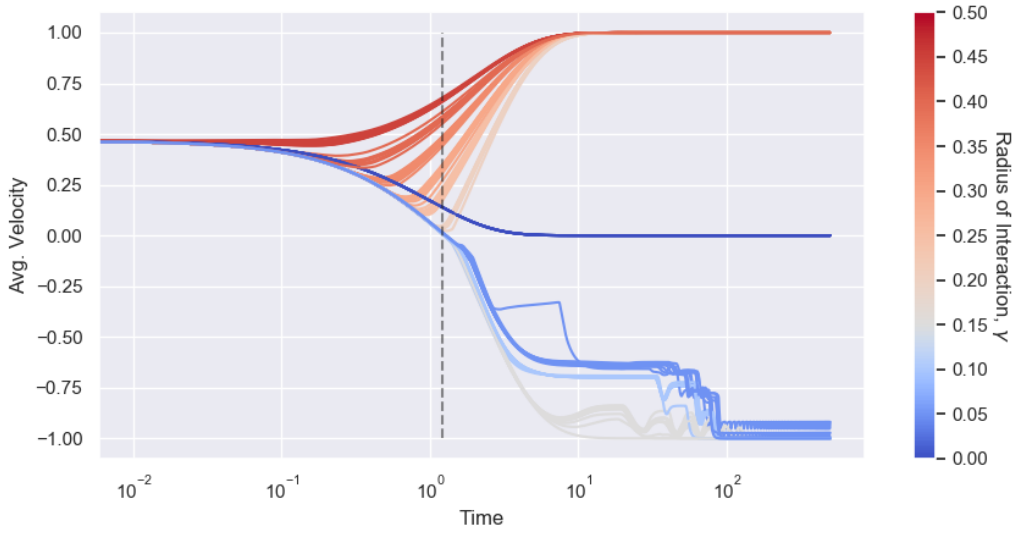

Figure 5: If the model is scaled globally, short interaction radii have a much larger convergence time. Here the system was evolved for 500s from an initial configuration of two clusters of uneven density. For higher interaction radii, behaviour is very similar. Some systems persist in a periodic trajectory for even larger times (tested up to 1000s). For corresponding heatmaps of convergence time, see Figure fig:2NNtau. Note the logarithmic scale.

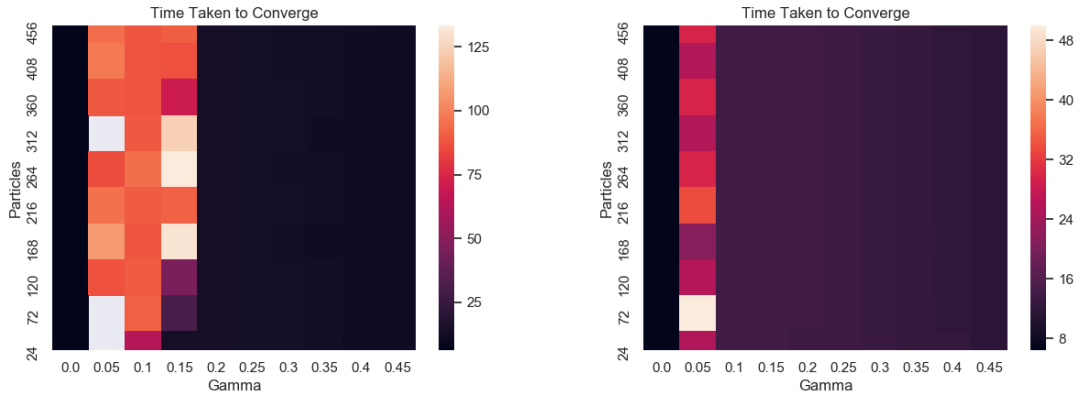

Figure 6: Time taken to converge for the local and global scaling. In the global case, values that did not converge within 500s have been represented as grey squares. We see the dependence on interaction radius for larger gamma and the independence of N in both cases. The chequerboard effect at intermediate values is caused by the randomness inherent in the initial spatial configuration. Note the difference in scale between the two subfigures.

	$N = 24$	$N = 168$	$N = 360$	$N = 456$
$\gamma = 0.05$	3	2	3	2
$\gamma = 0.15$	2	2	2	1
$\gamma = 0.3$	1	1	1	1
$\gamma = 0.45$	1	1	1	1

Table 1: Number of clusters remaining after $50s$ in the locally scaled system. Note that N has very little effect on the clustering while the radius of interaction does.

	$N = 24$	$N = 168$	$N = 360$	$N = 456$
$\gamma = 0.05$	1	1	1	1
$\gamma = 0.15$	1	1	1	1
$\gamma = 0.3$	1	1	1	1
$\gamma = 0.45$	1	1	1	1

Table 2: Number of clusters remaining after 500 in the globally scaled system. In contrast to the local system, only one cluster persists in any regime.

including stable states. The next step is to assess whether the clusters persist in any way in the particle system—a phenomenon we don't expect in the noisy system by +++P:product++. For this, we use the same initial condition.

4.2.1.4.2 Number of Clusters The number of clusters was assessed using histograms of the particles' positions at either $50s$ (in the locally scaled system) or $500s$ (in the globally scaled model). The longer time scale for the global case is so that the system has time to settle into a stable average velocity. Tables 1 and 2 summarise the result. In either case, a clustered pattern persists. This is intuitive in the deterministic model as there is no noise to break the clusters apart. Any dispersion can only arise through the interaction term, which will be approximately equal for two particles close together. For the local scaling, more clusters appear when γ is lower. When scaling globally however, there is always only one cluster remaining. This is perhaps because in the locally scaled model, for each cluster, the interaction is comparable due to the normalising effect of the denominator. In the globally scaled model, smaller clusters are penalised more heavily their interaction being reduced by the constant scaling by N. Smaller clusters thus get caught by larger clusters. This is not yet a contradiction of +++P:product+++, as we are only looking at the deterministic case, $\sigma = 0$.

4.2.1.4.3 Introducing Random Velocity Distributions Thus far, we have only considered deterministic initial velocities. Keeping the spatial initial condition the same, we instead assign initial velocities of particles in each cluster drawn from a normal distribution as follows

$$v^{i,3N} \sim \mathcal{N}(-0.2, 0.5^2) \quad \text{for } 1 \leq i \leq 2N,$$
$$v^{i,3N} \sim \mathcal{N}(1.8, 0.5^2) \quad \text{for } 2N \leq i \leq 3N.$$

The variance of the distributions was chosen here so that it was very unlikely that the average velocity of the whole cluster deviated too far from its mean value, thus approximately preserving the distance

from equilibria discussed earlier. Figure **??** shows the average velocities analogous to Figure 4 for this setup. For larger γ, the normally distributed does not affect the convergence compared to the deterministic initial velocity. In the local scaling, this indifference persists to lower γ. The only difference is for some intermediate radii, $\gamma \approx 0.2$, the system converges to $+1$ as opposed to -1. This however is only one realisation of the initial data. In the globally scaled case, the random velocity has more of an effect. Here it affects the convergence of both larger and smaller γ, with many systems oscillating close to ± 1.

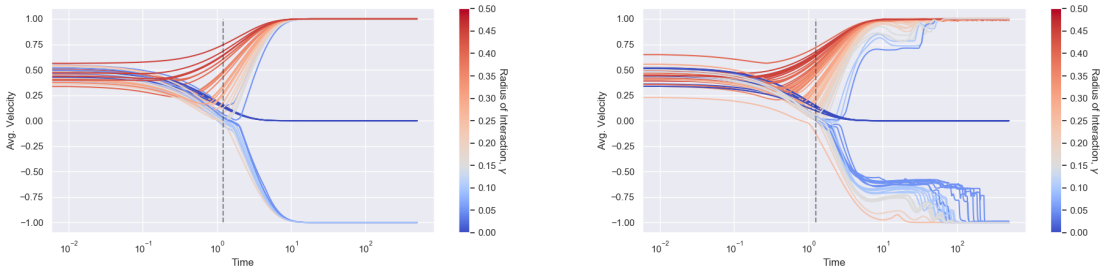

Figure 7: When the initial velocities are instead normally distributed instead of constant, we see different behaviour (c.f. Figure fig2NNavgvellocal,fig:2NNavgvelglobal). There is still a change in behaviour when the interaction radius is around 0.2, however it is much less well defined. The setup here is identical to Figure fig2NNavgvelglobal, other than the initial velocity distribution. We also see that some setups that previously converged to -1 converge to +1. Note that this is only one realisation of the initial configuration, upon averaging over many runs it should be similar to the deterministic initial condition.

Simplifying to the deterministic models illuminates the effects of different terms, without the effect of noise. We have seen here that the particle system average velocity is not monotone, and that it does not govern the equilibrium value. This has also made clear the difference in the two models, despite their similarity. In particular, the global scaling slows convergence for many different interaction radii compared to an identical locally scaled system.

5 Implementation

The majority of my work this year has been spent implementing these particle systems in Python. They are available online. There are currently three versions, and in this section each will be briefly described.

5.1 v0.1

Procedural

5.2 v0.2

OOP

5.3 v0.3

JIT compiled

stse

6 Future Work

PDE simulations, what else? What direction is the PhD going in?

[1] Xie, Y. (2016). *Bookdown: Authoring books and technical documents with R markdown.* Chapman; Hall/CRC, Boca Raton, Florida.

[2] Savill, N. J. and Hogeweg, P. (1997). Modelling morphogenesis: From single cells to crawling slugs. *Journal of Theoretical Biology* **184** 229–35.

[3] Schelling, T. C. (1971). Dynamic models of segregation. *The Journal of Mathematical Sociology* **1** 143–86.

[4] Hegselmann, R. and Krause, U. (2002). Opinion dynamics and bounded confidence: Models, analysis and simulation. *Journal of Artificial Societies and Social Simulation* **5** 1–24.

[5] Ballerini, M., Cabibbo, N., Candelier, R., Cavagna, A., Cisbani, E., Giardina, I., Orlandi, A., Parisi, G., Procaccini, A., Viale, M. and Zdravkovic, V. (2008). Empirical investigation of starling flocks: A benchmark study in collective animal behaviour. *Anim. Behav.* **76** 201–15.

[6] Buttà, P., Flandoli, F., Ottobre, M. and Zegarlinski, B. (2019). A non-linear kinetic model of self-propelled particles with multiple equilibria. *Kinetic & Related Models* **12(4)** 791–827.

[7] Vicsek, T., Czirók, A., Ben-Jacob, E., Cohen, I. and Shochet, O. (1995). Novel type of phase transition in a system of self-driven particles. *Phys. Rev. Lett.* **75** 1226–9.

[8] Cucker, F. and Smale, S. (2007). Emergent behavior in flocks. *IEEE Transactions on Automatic Control* **52** 852–62.

[9] Couzin, I. D., Krause, J., James, R., Ruxton, G. D. and Franks, N. R. (2002). Collective memory and spatial sorting in animal groups. *Journal of Theoretical Biology* **218** 1–11.

[10] Czirok, A., Barabasi, A.-L. and Vicsek, T. (1997). Collective motion of self-propelled particles: Kinetic phase transition in one dimension.

[11] Garnier, J., Papanicolaou, G. and Yang, T.-W. (2019). Mean field model for collective motion bistability. *Discrete & Continuous Dynamical Systems - B* **24** 851.